Available online at www.sciencedirect.com
ScienceDirect
Polymer 49 (2008) 1555–1561
polymer
www.elsevier.com/locate/polymer

High-pressure solution blending of poly(ε-caprolactone) with poly(methyl methacrylate) in acetone + carbon dioxide

Kun Liu, Erdogan Kiran*

Department of Chemical Engineering, Virginia Polytechnic Institute and State University, 132 Randolph Hall, Blacksburg, VA 24061, United States

Received 21 December 2007; received in revised form 29 January 2008; accepted 2 February 2008
Available online 8 February 2008

Abstract

The miscibility of blends of poly(ε-caprolactone) (PCL, $M_w = 14{,}300$) with poly(methyl methacrylate) (PMMA, $M_w = 15$K or 540K) in acetone + CO_2 mixed solvent has been explored. The liquid–liquid phase boundaries at different temperatures have been determined for mixtures containing 10 wt% total polymer blend, 50 wt% acetone and 40 wt% CO_2. The PCL and PMMA contents of the blends were varied while holding the total polymer concentration at 10 wt%. The polymer blend solutions all displayed LCST-type behavior and required higher pressures than individual polymer components for complete miscibility. Complete miscibilities were achieved at pressures within 40 MPa. The DSC scans show that the blends are microphase-separated. The blends display the melting transition of PCL and the glass transition temperature of the PMMA phases. The presence of PMMA is found to influence the crystallization and melting behavior of PCL in the blends. The DSC results on heat of melting and the FTIR spectra, specifically the changes at 1295 cm^{-1} band show the changes (decrease) in overall crystallinity of the blend upon addition of PMMA.
© 2008 Elsevier Ltd. All rights reserved.

Keywords: Poly(ε-caprolactone); Polymer blends; Supercritical carbon dioxide

1. Introduction

Polymer solution blending in high-pressure carbon dioxide or in fluid mixtures of carbon dioxide with an organic solvent is of continuing interest, and several publications have already appeared [1–5]. Specifically, the blends of poly(methyl methacrylate) and poly(ethyl methacrylate) were prepared from solutions in Freon-22 via rapid expansion of supercritical solutions [2]. The blends of polycarbonate with poly(styrene-*co*-acrylonitrile) were prepared from solutions in tetrahydrofuran (THF) by precipitation with carbon dioxide or heptane as anti-solvents [3]. The blends of isotactic polypropylene and poly(ethylene-*co*-butene) copolymers were also prepared in solutions of propane by rapid expansion [4]. Blends of PCL with PMMA have been prepared from solutions in dichloromethane by precipitation with carbon dioxide [6].

The interest in blends of PCL with other polymers stems from its biodegradability and their potential use in biomedical applications. It is used as a matrix for controlled-release drug system [7–9] or as materials for scaffolds in tissue engineering [10,11]. In biomedical application, the advantages of using PCL are linked to its slow degradation and its degradation products being neutral. Because of its low glass transition temperature ($T_g = -63$ °C [12]) along with its biodegradability, blends of PCL with other polymers have also been of interest. A comprehensive review covering the literature prior to 2000 is available [13]. It is used to lower the T_g of another polymer or enhance its degradation for environmental remediation. Indeed, blends of PCL have been reported at ambient pressures with poly(vinyl methyl ether), poly(styrene-*co*-acrylonitrile) [14], polypropylene [15], poly(L-lactic acid) [16], poly(butylene terephthalate) [17], tetramethyl polycarbonate [18] and polypyrrole [19]. PCL has also been explored as compatibilizer for polymer blends such as bisphenol polycarbonate with styrene–acrylonitrile copolymer [20].

* Corresponding author. Tel.: +1 540 231 1375; fax: +1 540 231 5022.
E-mail address: ekiran@vt.edu (E. Kiran).

0032-3861/$ - see front matter © 2008 Elsevier Ltd. All rights reserved.
doi:10.1016/j.polymer.2008.02.005

In contrast to PCL which is semi-crystalline, poly(methyl methacrylate) (PMMA) is an amorphous polymer also with a wide range of utilization areas, including biomedical implants such as replacement for intraocular lenses, bone cements, and dentures. Its blends have therefore been extensively studied as well. Among the recent publications are blends of PMMA with poly(vinylidene fluoride) [21,22], poly(L-lactic acid) [23,24], poly(vinyl chloride) [25–27], poly(ethylene terephthalate) [28,29], polystyrene (PS) [30], poly(styrene-*co*-acrylonitrile) [31] and poly(ethylene oxide) [32]. Studies on blending of PCL with PMMA is of special interest not only because of the potential modifications for biomedical applications or environmentally desirable attributes, but also because of the possibility of specific intermolecular interactions that may arise from the ester groups in the backbone of the PCL molecules and the ester groups in the side group in PMMA molecules. Even though such specific interactions have not been reported for blends of PCL with PMMA, interactions with other polymers are known. These include the interactions between carbonyl group (C=O) in PCL and PVC [33], poly(bisphenol A carbonate) [34], and poly(hydroxyl ether of bisphenol A) [35].

For effective design of pathways for solution blending, information on the phase behavior of the polymer mixtures is needed. This type of data is, however, extremely limited, especially for high-pressure solutions. The phase behavior of polyethylene + polypropylene blends in pentane [1] and the phase behavior of the blends of isotactic polypropylene and poly(ethylene-*co*-butene) copolymers in propane have been reported [4]. Studies on blends of semi-crystalline polymers with amorphous, glassy polymers are of additional interest in that the glassy polymers can alter the crystallization of the semi-crystalline polymers. In general, the presence of a glassy component leads to a crystallization depression of the crystallizable component due to either a reduction in chain mobility, or a dilution of the crystallizable component at the growth front, or a change in the free energy of nucleation [18,36]. In the presence of an amorphous component, lamellar thickness, crystal inter-phase, and the spherulitic growth rate of the crystallizable component are altered [18]. How these features are altered in dense fluids is not presently known.

In the present study, PMMA/PCL blends were prepared from their solutions in acetone + carbon dioxide mixtures at high pressures. We have recently reported on the properties of the acetone + CO_2 mixtures as tunable solvents [37]. We have also reported the phase behavior, viscosity, and density of PMMA solutions and PCL solutions in this mixture solvent at high pressures [38,39]. We now extend the phase behavior information from individual polymer solutions to the solutions of PCL + PMMA blends.

2. Experimental

2.1. Materials

The polymers PCL and PMMA were purchased from Scientific Polymer Products (Ontario, NY). The molecular weight (M_w) and polydispersity (PDI) of the PCL sample were 14,300 and 2.3, respectively. Two PMMA samples with different molecular weights ($M_w = 15K$, PDI = 1.8; and $M_w = 540K$, PDI = 2.8) were used. In the text and the figure captions, the molecular weights are expressed in shortened notations of 14K, 15K, and 540K. Acetone (Burdick & Jackson) with purity of 99.5% and CO_2 (Airgas) with a minimum purity of 99.9% were used without further purification.

2.2. Determination of liquid–liquid phase boundary

A variable-volume high-pressure view cell, described in our previous publications [40], was used to prepare the PCL/PMMA blends and to determine the liquid–liquid (L–L) phase boundaries in acetone + carbon dioxide mixtures at high pressures. After the polymers and the solvent with known amounts were charged, temperature and pressure were adjusted to achieve complete miscibility. The L–L phase boundary (demixing pressure) was then determined by decreasing the pressure at a given temperature while recording the transmitted light intensity, or visually observing the cell content through two sapphire windows. The pressure–temperature phase diagram was generated by repeating this miscibility/demixing pressure determination starting from homogeneous conditions at different temperatures.

2.3. Preparation of blends

In preparation of the blends, we followed the two-step process which is illustrated in Fig. 1. The first step is the depressurization at a given temperature to cross the liquid–liquid phase boundary. The second step is the further depressurization and cooling to ambient temperature. Typically, in the first stage, the pressure was decreased from about 20 MPa to around 6–7 MPa at a rate of 10 MPa/min. After holding the solution at the lower pressure (6–7 MPa) but still at the initial solution temperature (348 K) for 30 min with stirring, the system was completely depressurized by full discharge. The discharge was collected. The fraction not removed with expanding carbon dioxide during discharge and precipitates

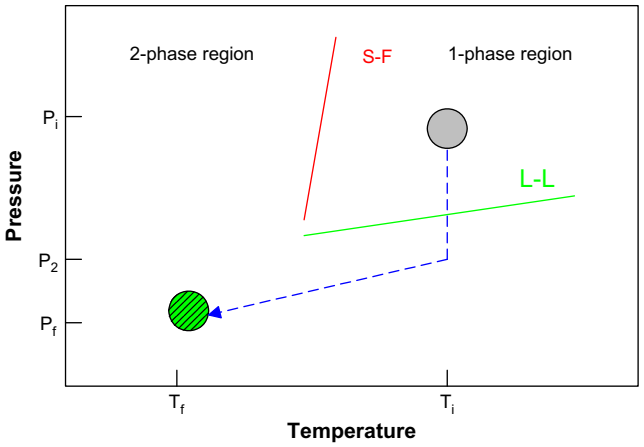

Fig. 1. The schematic of phase separation process in the formation of the blends.

in the view cell was dissolved in acetone and collected with the discharge. The solvent was evaporated by placing the samples in vacuum (0.05 Torr) for 72 h. Either powders or films were formed depending upon the composition of the blend. Film formation was enhanced in blends that contained higher fraction of PMMA. The polymer blends were then further characterized by DSC (in the temperature range from −50 to +150 °C) and FTIR (KBr disks were prepared using about 3 mg polymer samples).

3. Results and discussion

3.1. Liquid–liquid phase boundary

The liquid–liquid (L–L) phase boundaries were determined for 10 wt% PMMA ($M_w = 15K$; $M_w = 540K$), 10 wt% PCL ($M_w = 14K$), and 10 wt% (PMMA + PCL) blends. The amount of acetone and carbon dioxide in the solutions was maintained at 50 and 40 wt%, respectively. The blends with the low molecular weight PMMA were prepared with PCL concentrations of 2.5, 5.0, and 7.5 wt% (with PMMA concentrations being 7.5, 5 and 2.5%, respectively). In blends with the higher molecular weight PMMA, the PCL and PMMA concentrations were kept equal at 5 wt% each. The phase boundary data for these solutions are presented in Table 1 and Figs. 2–4.

Fig. 2 shows the liquid–liquid phase boundaries for the 10 wt% PCL ($M_w = 14K$), 10% PMMA ($M_w = 15K$) and the blends 10 wt% (PCL + PMMA) with PCL/PMMA mass ratios of 25/75, 50/50, and 75/25, respectively. All PCL containing solutions show higher L–L demixing pressures than the PMMA solutions at the same temperatures. All the blends display higher L–L demixing pressures than their corresponding polymer. Among these blends, even though the differences are slight, the 50/50 PCL/PMMA blend shows the highest demixing pressures and the 25/75 PCL/PMMA blend displays the lowest demixing pressures. In all the solutions, at given pressure, two-phase regions are entered when temperature is increased, a feature that is characteristic of systems showing LCST-type behavior.

Fig. 3 shows the L–L phase boundaries of 10 wt% PCL ($M_w = 14K$), the PMMA sample with the higher molecular weight ($M_w = 540K$), and their 50/50 blend solutions in acetone + carbon dioxide mixture. The solution of the high molecular weight PMMA shows higher demixing pressures than the pure PCL solution. However, once again, the 50/50 PCL/PMMA blend shows higher demixing pressures than the corresponding PCL or the PMMA solutions. A higher demixing pressure in blends is a consequence of the immiscibility of the polymer components. Indeed PCL and PMMA are known to be immiscible [41]. This recent manuscript which has explored the immiscibility of PMMA with a range of polyesters also provides an excellent perspective on the significance of these blends, and the role of the competition between crystallization and phase separation in altering the final morphology of these blends. The observation of higher demixing pressures in polymer blend solutions compared to their component solutions has been observed in other polymer systems such as the blends of polyethylene and polypropylene in pentane [1]. Polyethylene and polypropylene are also incompatible. Fig. 4 shows the phase boundaries for the solutions of the 50/50 blends of PCL with PMMA for the low and high molecular weight polymer samples. The blend with higher molecular weight PMMA displayed higher demixing pressures.

3.2. Polymer blend characterizations

3.2.1. Differential scanning calorimetric (DSC) results

The DSC scans were carried out at 10 K/min heating and cooling rates. The glass transition temperatures of the PMMA samples were determined to be 80 and 120 °C for the low (15K) and high (540K) molecular weight samples, respectively. Fig. 5 shows the DSC scan for PCL. A double melting transition is displayed with peak temperatures at 54.5 and 57 °C. The blends all displayed similar double melting transitions. They are shown in Fig. 6. This figure also shows the reduction in heat of melting (displayed by the area under the melting curve) with decreasing amount of PCL in the blends.

Fig. 7 shows the cooling scans immediately after the first heating scans displaying the crystallization peaks. The 50/50 and the 25/75 PCL/PMMA blends showed distinct multiple crystallization peaks. The heats of crystallization assessed from total peak areas are given in Table 2. The heat of crystallization and melting values show some differences. The slightly lower heats of crystallization may be due to the compositional effect or influence of PMMA in reducing the degree of crystallization of PCL in the blends. The heat of crystallization data suggest PCL compositions in the blends to be 67, 36, and 14 wt%, as compared to 75, 50, and 25 wt% initial mixture compositions loaded into the view cell. If the heat of melting data are used, the results suggest blend compositions of 67, 42, and 13 wt%. It should, however, be noted that since the degree of crystallization of PCL is decreased (as reflected by the lower heats of crystallization), heat of crystallization data cannot be directly used to calculate the PCL content in the blends. For the high molecular weight PMMA blends, both the heats of melting and crystallization lead to 40 wt% PCL in blends.

Fig. 8 combines the crystallization temperature for the polymer blends and the L–L demixing temperatures at 15 and 20 MPa (from Fig. 2) of the PCL ($M_w = 14K$)/PMMA ($M_w = 15K$) blends in acetone + carbon dioxide mixture. The figure illustrates the variation of demixing and crystallization temperatures with the PCL content. In this figure, the data points corresponding to 0% PCL represent the L–L demixing temperatures of pure PMMA solutions at 15 and 20 MPa. The data points corresponding to 100% PCL represent the L–L demixing temperatures of pure PCL solutions in acetone + carbon dioxide at 15 and 20 MPa, and the crystallization temperature of PCL at ambient pressure, shown as T_c*. The regions above the demixing temperature curves correspond to L–L phase-separated regions. The variation of crystallization temperature with PCL concentration shows that the addition of PMMA results in a decrease (even though small) in the crystallization temperature of these blends.

Table 1
Demixing pressures at different temperatures for 10 wt% PCL ($M_w = 14{,}300$), PMMA ($M_w = 15{,}000$ or 540,000), and their blend solutions in acetone + carbon dioxide mixtures

Temperature (K)	Pressure (MPa)
PCL ($M_w = 14{,}300$) (10 wt%) + acetone (50 wt%) + carbon dioxide (40 wt%)	
325.0	4.9
330.0	6.8
337.6	9.1
342.5	10.5
347.5	11.9
352.8	12.7
356.8	14.7
363.5	16.7
369.3	18.4
374.0	19.5
380.1	21.1
384.9	22.4
389.0	23.3
394.5	24.7
399.4	26.0
PMMA ($M_w = 15{,}000$) (10 wt%) + acetone (50 wt%) + carbon dioxide (40 wt%)	
347.1	10.5
352.0	11.5
356.0	13.0
360.3	14.0
366.5	15.4
370.0	16.5
374.8	18.0
380.4	19.0
385.4	21.0
390.0	22.0
393.3	23.0
399.1	24.5
PCL ($M_w = 14{,}300$) (2.5 wt%) + PMMA ($M_w = 15{,}000$) (7.5 wt%) + acetone (50 wt%) + carbon dioxide (40 wt%)	
341.1	10.5
347.0	12.6
353.4	14.3
358.0	15.7
363.3	17.2
368.5	18.6
374.1	20.3
379.5	21.7
384.9	23.2
390.9	24.5
395.3	25.4
400.8	27.0
PCL ($M_w = 14{,}300$) (5 wt%) + PMMA ($M_w = 15{,}000$) (5 wt%) + acetone (50 wt%) + carbon dioxide (40 wt%)	
326.1	7.5
333.1	9.7
337.4	10.9
343.8	13.0
347.5	14.3
354.8	16.0
359.8	17.3
365.5	19.2
370.1	20.4
375.5	22.0
380.6	23.0
384.9	24.2
390.4	25.6
394.3	26.4
400.6	27.8
PCL ($M_w = 14{,}300$) (7.5 wt%) + PMMA ($M_w = 15{,}000$) (2.5 wt%) + acetone (50 wt%) + carbon dioxide (40 wt%)	
328.0	7.1
332.8	8.5
339.0	10.5
344.0	12.2
351.5	14.5
356.1	15.8
362.3	17.5
369.0	19.5
374.1	20.6
377.4	22.0
379.4	22.4
384.6	23.8
389.8	24.9
394.6	26.1
401.0	27.6
PMMA ($M_w = 540{,}000$) (10 wt%) + acetone (50 wt%) + carbon dioxide (40 wt%)	
330.0	15.5
335.5	17.0
340.5	18.5
348.3	20.0
353.1	22.0
359.0	23.5
365.4	24.5
370.1	25.5
376.0	27.0
381.9	28.5
386.6	29.5
391.9	30.5
396.4	32.5
400.4	34.0
PCL ($M_w = 14{,}300$) (5 wt%) + PMMA ($M_w = 540{,}000$) (5 wt%) + acetone (50 wt%) + carbon dioxide (40 wt%)	
352.3	23.0
356.5	24.0
363.3	26.0
367.6	27.0
372.8	29.0
373.4	29.3
378.8	30.5
384.0	32.0
389.5	34.0
395.1	35.0
400.1	37.0

Fig. 8 is a rare diagram displaying the actual crystallization data and L–L demixing conditions in a common plot for a blend system prepared from high-pressure solutions displaying LCST-type behavior. These types of diagrams for high-pressure polymer solutions are not common in the literature yet would be of great significance in providing direct information on the temperature below which the system must be quenched to bring about Solid–Fluid (S–F) phase separation when homogeneous solutions are expanded. Ideally one should include the crystallization temperature at high pressure in the presence of the solvent [T_c(S–F)] along with the ambient pressure crystallization curve. However, in our experimental system, we do not have the

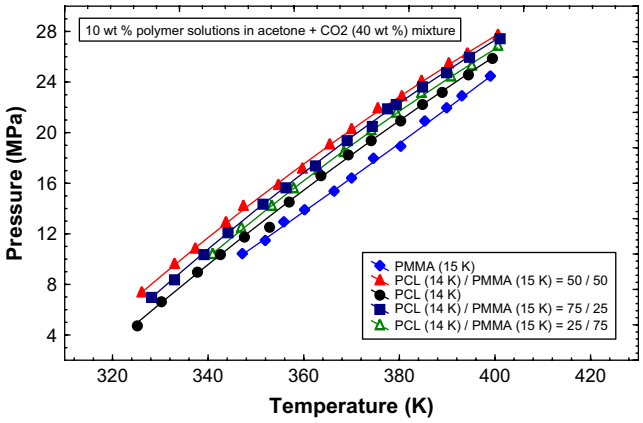

Fig. 2. Variation of demixing pressure with temperature for 10 wt% PCL, PCL/PMMA blends, and PMMA (15K) solutions in acetone (50 wt%) + carbon dioxide (40 wt%) mixture. Molecular weight: $M_w = 14$K (PCL); 15K (PMMA).

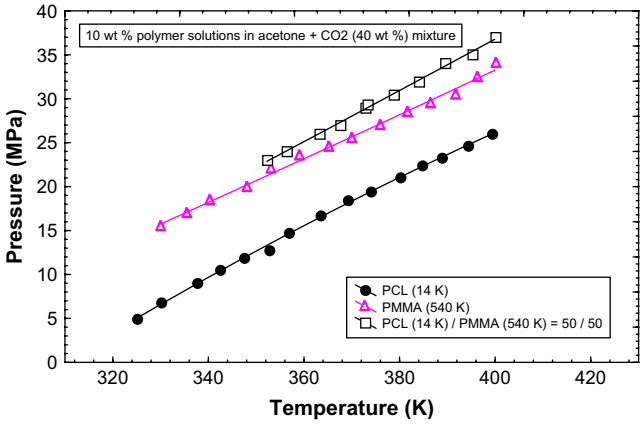

Fig. 3. Variation of demixing pressure with temperature for 10 wt% PCL (14K), PCL (14K)/PMMA (540K) blend, and PMMA (540K) solutions in acetone (50 wt%) + carbon dioxide (40 wt%) mixture.

capability to cool the view cell to sub-ambient temperatures. In systems where the S–F phase boundary remains at temperatures above the ambient temperature even in the presence of a solvent, such as polyethylene + pentane system, we have in the past shown that the crystallization boundary is shifted to

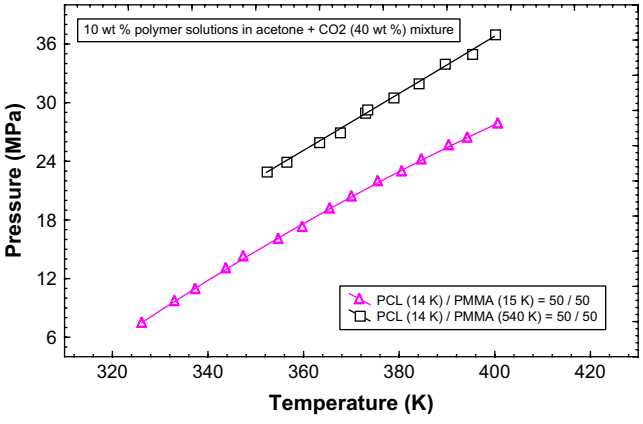

Fig. 4. Variation of demixing pressure with temperature for solutions of 5 wt% PCL (14K) + 5 wt% PMMA (15K) and 5 wt% PCL (14K) + 5 wt% PMMA (540K) in acetone (50 wt%) + carbon dioxide (40 wt%) mixture.

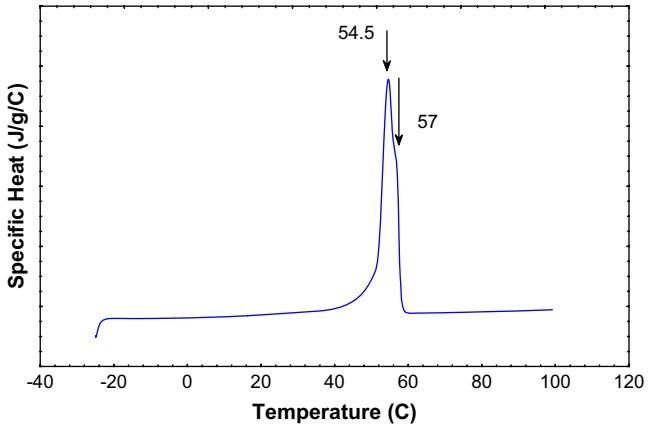

Fig. 5. First heating scan for original PCL sample ($M_w = 14$K).

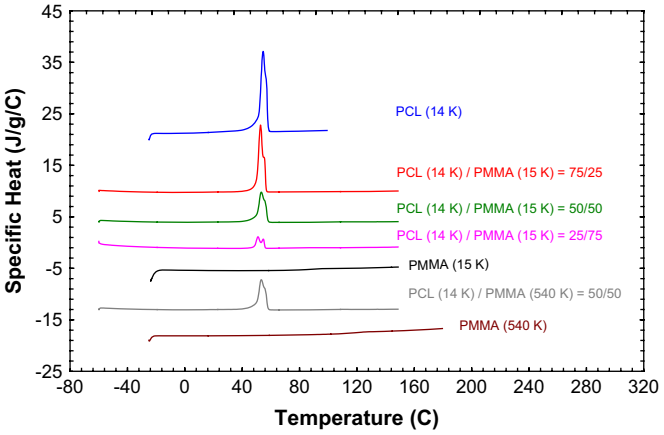

Fig. 6. Comparative DSC scans (first heating scans) for PCL ($M_w = 14$K), PMMA ($M_w = 15$K), PMMA ($M_w = 540$K) and their blends.

lower temperatures [40,42,43], and shows a small pressure dependence, with crystallization temperatures becoming higher at higher pressures. The net effect of solvent and pressure is, however, a lowered crystallization temperature. To further highlight the expected shift to lower temperatures in the presence of a solvent, a generalized diagram is included as an inset in Fig. 8 where T_c(S–F) boundary represents the crystallization curve in the presence of the solvent, and T_c* represents the ambient

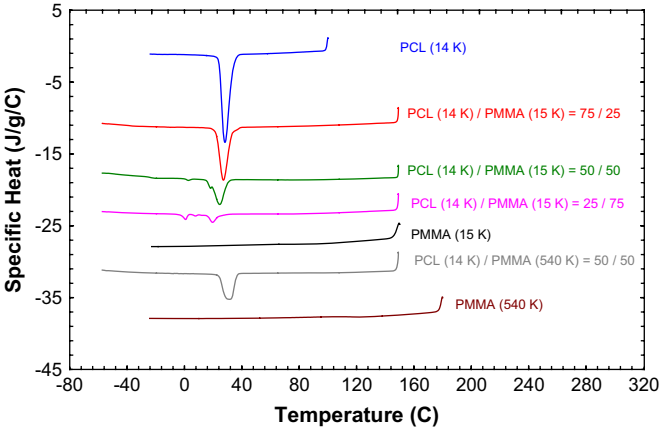

Fig. 7. Comparative DSC scans (first cooling scans) for PCL ($M_w = 14$K), PMMA ($M_w = 15$K), PMMA ($M_w = 540$K) and their blends.

Table 2
Melting and crystallization temperatures, and heats of melting and crystallization for PCL ($M_w = 14{,}300$) and its blends with PMMA ($M_w = 15{,}000$ or 540,000)

Polymer or polymer blends	Cooling scan		Heating scan	
	Heat of crystallization[a] (J/g)	Crystallization temperature[b] (°C)	Heat of melting[a] (J/g)	Melting temperature[b] (°C)
PCL (14K)	78	28	84	54.5, 57
PCL(14K)/PMMA (15K)				
75/25	52	27	57	54, 57
50/50	28	−22, 2, 18, 24	36	53, 57
25/75	11	0, 8, 12, 20	11	51, 55
PCL(14K)/PMMA (540K)				
50/50	30	30, 32.5	35	53, 56

[a] Peak areas are based on total peak area including all peaks.
[b] Transition temperatures are included only for the major peaks that are distinct.

pressure solvent-free crystallization temperatures. Along the direction of the arrows, phase separation will occur upon either increasing or decreasing the temperature. What is important to realize is that the nature of the phase separation will be different along the paths that accompany an increase or a decrease in temperature. Starting at homogeneous conditions, increasing the temperature leads to L–L phase separation, but lowering the temperature leads to S–F phase separation.

3.2.2. FTIR tests

Fig. 9 shows the IR spectra for PCL, PMMA and their blends. Fig. 10 is an expansion of the region from 600 to 2000 cm^{-1} which shows the changes in the band at 1295 cm^{-1}. The IR spectral features of PCL and PMMA are available in the literature [44,45]. In the PCL spectrum, the bands in the range 2867–2947 cm^{-1} are assigned to $-CH_2$ stretching, the band at 1727 cm^{-1} is assigned to the C=O carbonyl stretching, the band at 1295 cm^{-1} is assigned to C–O and C–C stretching in the crystalline phase, and the band at 1241 cm^{-1} is assigned to asymmetric COC stretching [41]. The band at 1295 cm^{-1} has been used in the literature to investigate the crystallinity

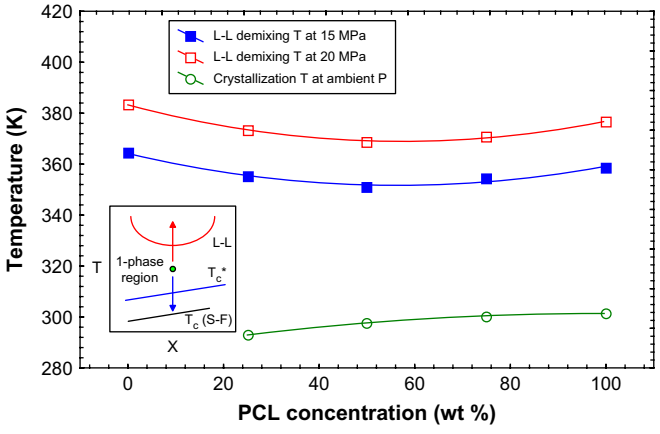

Fig. 8. Variation of liquid–liquid phase boundary with PCL concentration for PCL ($M_w = 14$K) + PMMA (15K) blend (10 wt% total polymer) solutions in acetone (50 wt%) + carbon dioxide (40 wt%) at 15 and 20 MPa. The ambient pressure crystallization temperatures of the PCL + PMMA blends in the absence of solvent are also included. This is depicted as T_c* in the inset figure. T_c(S–F) at lower T represents the crystallization curve in the presence of solvent fluid. Starting at homogeneous conditions, increasing the temperature leads to L–L phase separation, and lowering the temperature leads to S–F phase separation.

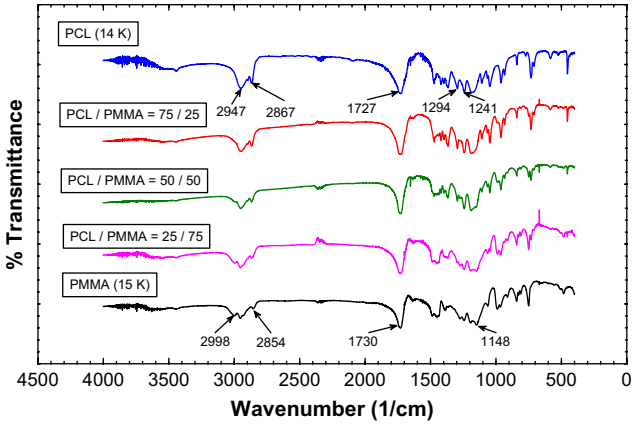

Fig. 9. Comparison of FTIR spectra for PCL ($M_w = 14$K), PMMA ($M_w = 15$K), and their blends.

change in PCL [44]. In the PMMA spectrum, the bands in the range 2854–2998 cm^{-1} are assigned to C–H stretching, the band at 1730 cm^{-1} is assigned to the C=O carbonyl stretching, and the band at 1148 cm^{-1} is assigned to $-OCH_3$ stretching [45]. These bands were verified with the PCL and PMMA samples used in the present study. The band at 1295 cm^{-1} corresponding to the C–O and C–C stretching in the crystalline phase shows a decrease with inclusion of glassy PMMA in the blend and eventually disappears in the pure PMMA spectrum,

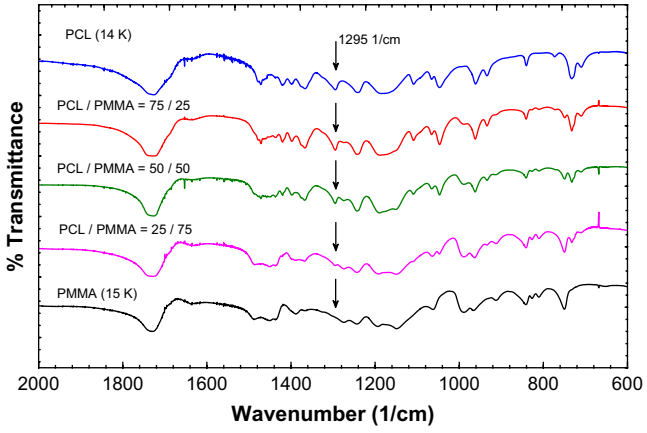

Fig. 10. Comparison of FTIR spectra for PCL ($M_w = 14$K), PMMA ($M_w = 15$K), and their blends in the wavenumber range 600–2000 cm^{-1}. The band at 1295 cm^{-1} is used to characterize the crystallinity of PCL and its blends with PMMA.

demonstrating the transformation from PCL to PMMA. The IR spectra confirm the formation of PCL + PMMA blends. The spectra do not show any new bands in the blends that can be associated with some specific interactions between PCL and PMMA, thus suggesting the absence of specific interactions in these blends.

4. Summary and conclusions

For the first time miscibility boundaries for blends of PCL and PMMA in acetone + carbon dioxide mixtures have been determined at high pressures. The solutions all show LCST-type phase behavior and polymer blends require higher pressures than the solutions of constituent polymers PMMA and PCL to bring about complete miscibility. The DSC results indicate that the blends are microphase-separated blends that display both the T_g of PMMA and T_m/T_c of PCL. The FTIR tests confirm the formation of polymer blends and the changes in the band at 1295 cm^{-1} confirm the changes (decrease) in PCL crystallinity upon addition of PMMA.

References

[1] Kiran E. Supercritical fluids: fundamentals for application. Dordrecht: Kluwer Academic Publishers; 1994.
[2] Lele AK, Shine AD. Industrial and Engineering Chemistry Research 1994;33:1476–85.
[3] Mawson S, Kanakia S, Johnston KP. Polymer 1997;38(12):2957–67.
[4] Han SJ, Lohse DJ, Radosz M, Sperling LH. Journal of Applied Polymer Science 2000;77:1478–87.
[5] Duarte ARC, Gordillo MD, Cardoso MM, Simplicio AL, Duarte CMM. International Journal of Pharmaceutics 2006;311:50–4.
[6] Vega-Gonzalez A, Domingo C, Elvira C, Subra P. Journal of Applied Polymer Science 2004;91:2422–6.
[7] Xie JW, Marijnissen JCM, Wang CH. Biomaterials 2006;27(17): 3321–32.
[8] Wu B, Borland SW, Giordano RA, Cima LG, Sachs EM, Cima MJ. Journal of Controlled Release 1996;40(1–2):77–87.
[9] Lin WJ, Yu CC. Journal of Microencapsulation 2001;18(5):585–92.
[10] Reignier J, Huneault MA. Polymer 2006;47(13):4703–17.
[11] Sarkar S, Lee GY, Wong JY, Desai TA. Biomaterials 2006;27(27): 4775–82.
[12] Jin S, Gonsalves KE. Macromolecules 1997;30:3104–6.
[13] Eastmond GC. Advances in Polymer Science 2000;149:59–223.
[14] Men Y, Strobl G. Macromolecules 2003;36:1889–98.
[15] Balsamo V, Gouveia L. e-Polymers 2004;17:1–19.
[16] Tanaka T, Tsuchiya T, Takahashi H, Taniguchi M, Lloyd DR. Desalination 2006;193:367–74.
[17] Di Lorenzo ML, La Pietra P, Errico ME, Righetti MC, Angiuli M. Polymer Engineering and Science 2007:323–9.
[18] Madbouly SA. Journal of Applied Polymer Science 2007;103:3307–15.
[19] Corres MA, Mugica A, Carrasco PM, Cortazar MM. Polymer 2006;47:6759–64.
[20] Deanin RD, Vale T. Polymeric Materials Science and Engineering 2000;83:388.
[21] Lin AJ, Chang CL, Lee CK, Cheng LP. European Polymer Journal 2006;42:2407–18.
[22] Ma WZ, Zhang J, Wang XL, Wang SM. Applied Surface Science 2007;253:8377–88.
[23] Hirota S, Sato T, Tominaga Y, Asai S, Sumita M. Polymer 2006;47:3954–60.
[24] Yao BS, Nawaby AV, Liao X, Burk R. Journal of Cellular Plastics 2007;43:385–98.
[25] Zhuo C, Si QB, Ao YH, Tan ZY, Sun SL, Zhang MY, et al. Polymer Bulletin 2007;58:979–88.
[26] Agari Y, Anan Y, Nomura R, Kawasaki Y. Polymer 2007;48:1139–47.
[27] Aouachria K, Belhaneche-Bensemra N. Polymer Testing 2006;25: 1101–8.
[28] Al-Mulla A, Shaban HI. Polymer Bulletin 2007;58:893–902.
[29] Al-Mulla A. Express Polymer Letters 2007;1(6):334–44.
[30] Kailas L, Bertrand P. Applied Surface Science 2006;252:6648–51.
[31] Prusty M, Keestra BJ, Goossens JGP, Anderson PD. Chemical Engineering Science 2007;62:1825–37.
[32] Okerberg BC, Marand H. Journal of Materials Science 2007;42:4521–9.
[33] Coleman MM, Zarian J. Journal of Polymer Science: Polymer Physics Edition 1979;17:837–50.
[34] Varnell DF, Runt JP, Coleman MM. Macromolecules 1981;14:1350–6.
[35] Coleman MM, Moskala EJ. Polymer 1982;24:251–7.
[36] Ajili SH, Ebahimi NG. Macromolecular Symposium 2007;249–259:623–7.
[37] Liu K, Kiran E. Industrial and Engineering Chemistry Research 2007;46:5453–62.
[38] Liu K, Schuch F, Kiran E. Journal of Supercritical Fluids 2006;39: 89–101.
[39] Liu K, Kiran E. Journal of Supercritical Fluids 2006;39:192–200.
[40] Zhang W, Kiran E. Journal of Supercritical Fluids 2006;38:406–19.
[41] Li SH, Woo EM. Colloid Polymer Science, in press (doi:10.1007/s00396-007-1762-1).
[42] Upper G, Zhang W, Beckel D, Shon S, Liu K, Kiran E. Industrial and Engineering Chemistry Research 2005;45:1478–92.
[43] Fang J, Kiran E. Journal of Supercritical Fluids 2006;38:132–45.
[44] Elzein T, Nasser-Eddine M, Delaite C, Bistac S, Dumas P. Colloid and Interface Science 2004;273:381–7.
[45] Ramesh S, Leen KH, Kumatha K, Arof AK. Spectrochimica Acta, Part A 2007;66:1237–42.